Human Molecular Genetics, 2013, Vol. 22, No. 2 **372–383**
doi:10.1093/hmg/dds434
Advance Access published on October 25, 2012

A critical role for Telethonin in regulating t-tubule structure and function in the mammalian heart

Michael Ibrahim[1,2], Urszula Siedlecka[1], Byambajav Buyandelger[3], Mutsuo Harada[4], Christopher Rao[1], Alexey Moshkov[2], Anamika Bhargava[2], Michael Schneider[4], Magdi H. Yacoub[1], Julia Gorelik[2], Ralph Knöll[3,†] and Cesare M. Terracciano[1,*,†]

[1]Laboratory of Cell Electrophysiology, Heart Science Centre, Harefield Hospital, London UB9 6JH, UK [2]Laboratory of Functional Microscopy, Myocardial Function Section, [3]Laboratory of Myocardial Genetics, and [4]Laboratory of Cardiac Myogenesis, Death and Regeneration, Heart Science Section, National Heart and Lung Institute, Imperial College London, London, UK

Received June 8, 2012; Revised and Accepted October 8, 2012

The transverse (t)-tubule system plays an essential role in healthy and diseased heart muscle, particularly in Ca^{2+}-induced Ca^{2+} release (CICR), and its structural disruption is an early event in heart failure. Both mechanical overload and unloading alter t-tubule structure, but the mechanisms mediating the normally tight regulation of the t-tubules in response to load variation are poorly understood. Telethonin (Tcap) is a stretch-sensitive Z-disc protein that binds to proteins in the t-tubule membrane. To assess its role in regulating t-tubule structure and function, we used Tcap knockout (KO) mice and investigated cardiomyocyte t-tubule and cell structure and CICR over time and following mechanical overload.In cardiomyocytes from 3-month-old KO (3mKO), there were isolated t-tubule defects and Ca^{2+} transient dysynchrony without whole heart and cellular dysfunction. Ca^{2+} spark frequency more than doubled in 3mKO. At 8 months of age (8mKO), cardiomyocytes showed progressive loss of t-tubules and remodelling of the cell surface, with prolonged and dysynchronous Ca^{2+} transients. Ca^{2+} spark frequency was elevated and the L-type Ca^{2+} channel was depressed at 8 months only.

After mechanical overload obtained by aortic banding constriction, the Ca^{2+} transient was prolonged in both wild type and KO. Mechanical overload increased the Ca^{2+} spark frequency in KO alone, where there was also significantly more t-tubule loss, with a greater deterioration in t-tubule regularity. In conjunction, Tcap KO showed severe loss of cell surface ultrastructure. These data suggest that Tcap is a critical, load-sensitive regulator of t-tubule structure and function.

INTRODUCTION

T-tubule dysfunction is a major feature of cardiac diseases and occurs early in heart failure (HF) (1). A major biophysical regulator of t-tubule structure appears to be mechanical load variation, with both increases (1) and decreases (2) in mechanical load altering the t-tubule structure. Furthermore, the treatment of HF-induced overload with mechanical unloading can reverse t-tubule dysfunction (3), indicating that this is a reversible phenomenon. Therefore, the t-tubule system is tightly regulated by load variation in both health and disease.

The t-tubules are membrane invaginations that contain high density of L-type Ca^{2+} channels and allow tight coupling with RyR (4). They have a number of important physiological functions, most importantly in promoting synchronous Ca^{2+} transients and efficient contraction (5).

A number of molecules are implicated in t-tubule regulation (1,6–8). However, these mechanisms have not been linked to load variation. Tcap encodes a 19 KDa protein located in the Z-disc (9) and is a candidate load-dependent regulator of t-tubule structure because it (i) is a part of the stretch-sensitive complex of the cardiomyocyte Z-disc (10), (ii) it links this

*To whom correspondence should be addressed at: Harefield Heart Science Centre, Imperial College London, London UB9 6JH, UK. Tel: +44 1895453874; Fax +44 1895828900; Email: c.terracciano@imperial.ac.uk
†These authors contributed equally.

stretch-sensitive complex with proteins in the t-tubule membrane (11), (iii) is stretch sensitive in expression and is required for normal t-tubule development in zebrafish skeletal muscle (12) and (iv) is mutated in a manner that increases stretch sensitivity in hypertrophic cardiomyopathy and in a manner that reduces stretch sensitivity in dilated cardiomyopathy (13), conditions where t-tubule abnormalities also exist (14). It is known that Tcap plays an important role in the response to cardiac overload. Using a mouse model, we showed that the knockout (KO) of Tcap is associated with no spontaneous whole-heart phenotype, including preserved contractility (15). After mechanical overload, cardiac dysfunction occurs with pronounced apoptosis (15). In particular, Zhang *et al.'s* study (12) suggested that Tcap might be a load-dependent molecular regulator of the t-tubule membrane in the skeletal muscle.

Based on these studies, we hypothesize that Tcap is a load-dependent regulator of t-tubule structure in the heart. T-tubule structure was examined using Di-8-ANEPPS staining, and the cell surface structure was examined using scanning ion conductance microscopy (SICM). Ca^{2+} handling was assessed using confocal laser microscopy and patch clamping techniques.

RESULTS

Lack of Tcap brings about progressive Ca^{2+} handling defects

In isolated LV myocytes, we first assessed the whole-cell Ca^{2+} transient during ageing. We chose to study two time points, 3 months of age, corresponding to young mice that were previously described (15) and 8 months of age. In 3-month-old KO (3mKO), the gross features of the Ca^{2+} transients had a normal time to peak, amplitude and time for 50 and 90% decline. This is consistent with the previous description of the Ca^{2+} transient in this Tcap KO model (15). We also sought to analyse the synchrony of the Ca^{2+} transient, which is tightly related to the structural integrity of the t-tubule network (16). We calculated the variance of the time to peak, a measure of the synchrony of Ca^{2+} release across the length of the cell, that was increased at 3mKO, indicating impaired Ca^{2+} release synchrony, possibly related to irregular t-tubule structure (Fig. 1). In 8mKO, we observed more extensive changes with remodelling of the Ca^{2+} transient. The time to peak of the Ca^{2+} transient was increased, and the time for 90% (but not 50%) decline was also prolonged. The amplitude of the Ca^{2+} transient was unaffected at both 3 and 8 months.

We further investigated the mechanisms that may be responsible for the changes to the whole-cell Ca^{2+} transient. Ca^{2+} sparks are quiescent Ca^{2+} fluxes from clusters of RyRs and are the functional constituents of the Ca^{2+} transients (17). We found that, in 3mKO and 8mKO, there was an elevated Ca^{2+} spark frequency, the cardinal sign of sarcoplasmic reticulum (SR) Ca^{2+} leak. Such changes are commonly observed in cardiomyocytes that show t-tubule irregularity (2,3,5). There was an associated reduction in Ca^{2+} spark peak amplitude (Fig. 2). This indicates impaired SR Ca^{2+} release function that could be due to altered L-type Ca^{2+} channel (LTCC) activity, dyadic disruption or primary changes to the RyR. We found no difference in LTCC density in 3mKO myocytes; however, myocytes from 8mKO had a significant reduction in LTCC density (Fig. 2). Such a reduced LTCC density might be expected to reduce stimulation of the RyRs, and this, therefore, makes the LTCC an unlikely cause for such changes. The action potential (AP) was unchanged in amplitude or time for 50 and 90% depolarization (Supplementary Material, Fig. S1). Changes to the AP can alter Ca^{2+} release synchrony, (18) and it is important to exclude this as a cause of such changes in this study.

T-tubule and cell surface structure was disrupted in Tcap KO

We investigated whether the isolated loss of Ca^{2+} transient synchronicity in myocytes from 3mKO could be due to pathological changes to the t-tubule system. In 3mKO, we found that there was a normal density of the t-tubules. However, it is known that structural irregularities (rather than loss) of the t-tubule system alone are sufficient to induce delayed zones of Ca^{2+} release. Using the power index of the Fourier transform as an index of the t-tubule regularity, we found that the t-tubules were structurally irregular (Fig. 3). In 8mKO, the t-tubule abnormalities had progressed, with the loss of both t-tubule density and regularity (Fig. 3).

T-tubules are invaginations of the cell membrane, with which they form a sophisticated electrophysiological complex. To study the structure of the cell surface, we used SICM. We found that 3mKO had a normal cell surface structure with a typical pattern of fine membrane striations (Z-grooves) in which orderly t-tubules reside (Fig. 4). However, in 8mKO, there was loss of the fine membrane architecture with a reduced Z-groove index (Fig. 4). This pattern of changes has been described in HF of multiple aetiologies, where there is also derangement of the t-tubule network (14).

In unstressed hearts, therefore, there is a subtle loss of t-tubule structural regulation, which results in a typical pattern of t-tubule-related Ca^{2+} handling abnormalities.

Mechanical overload caused marked Ca^{2+} handling abnormalities in Tcap KO

To assess the impact of chronic mechanical overload on t-tubule structure in the absence of Tcap, we subjected Tcap KO and wild-type (WT) mice to thoracic aortic constriction (TAC). After chronic mechanical overload induced by TAC for 4 weeks in 3 months old mice, both WT and KO cells showed prolongation of the time to peak and increased variance of time to peak (Fig. 5). The Ca^{2+} handling abnormalities in Tcap KOs were more pronounced, with a greater increase in the variance of the time to peak than WT, and additional prolongation of the time for 50 and 90% decline of the Ca^{2+} transient, indicating a more pronounced loss of normal Ca^{2+} handling. It is noteworthy that in some studies of mechanical overload, significantly defective Ca^{2+} handling is found (19), whereas in others, mechanical overload-induced remodelling of the local Ca^{2+}-induced Ca^{2+} release (CICR) apparatus appears to be compensated for, resulting in few Ca^{2+} handling and whole-heart changes (1,20). This indicates that the present model of mechanical overload lies at the severe end of the spectrum.

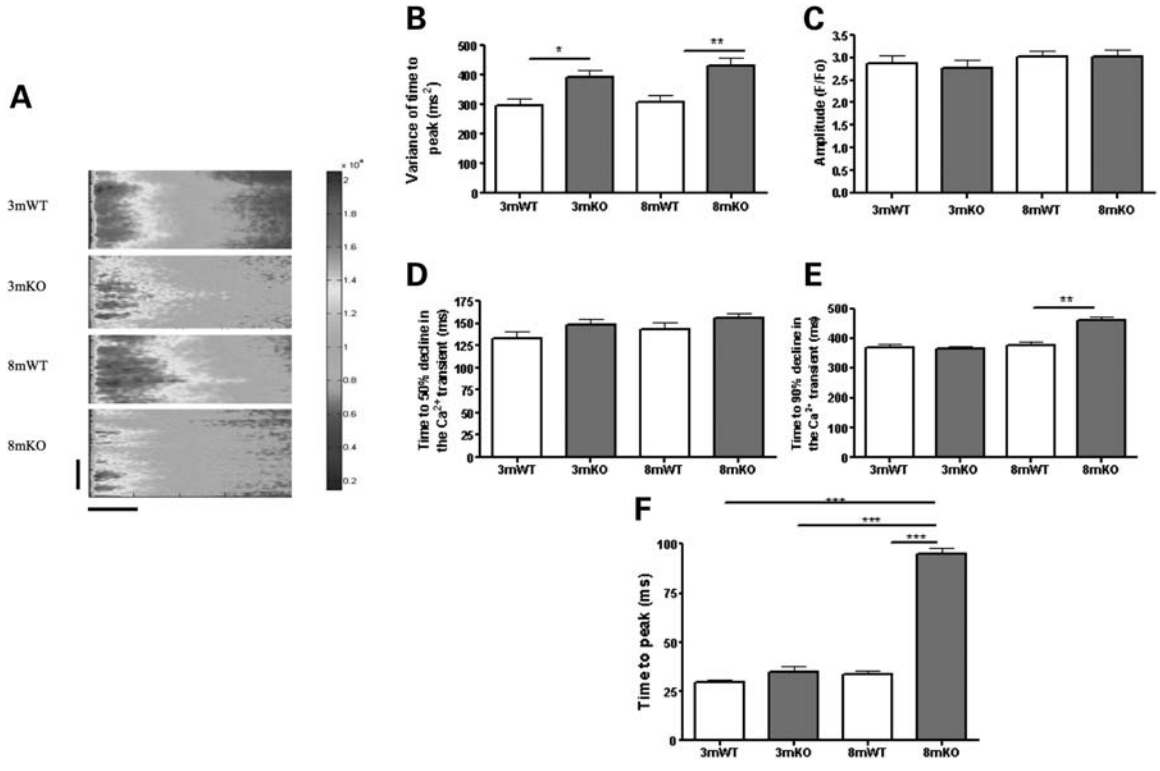

Figure 1. Tcap KO is associated with progressive Ca^{2+} transient defects. (**A**) The figure shows line scans of stimulated ventricular cardiomyocytes from 3 months old or 8 months old WT and Tcap KO hearts. The colour chart is a normalized scale of fluorescence intensity (a marker of Ca^{2+} concentration). 3mWT $n = 40$, 3mKO $n = 48$, 8mWT $n = 48$, 8mKO $n = 43$. The vertical scale bar represents 100 pixels and the horizontal scale bar represents 100 ms. Variance of time to peak (**B**), amplitude (**C**) and time for 50% (**D**) and 90% (**E**) decline and the time to peak (**F**) of the Ca^{2+} transient were deleteriously affected in the KO. Importantly, the variance of the time to peak (which is closely associated with changes to the t-tubules) was the only parameter influenced at 3 m.

To understand the mechanisms involved in the Ca^{2+} transient abnormalities in response to TAC, we studied Ca^{2+} spark properties. KO, but not WT, cells showed increased Ca^{2+} spark frequency (Fig. 6), a possible feature of dyadic dysregulation (5). There was also a slight prolongation of the Ca^{2+} spark duration in both WT and KO cells after TAC. The Ca^{2+} spark duration was increased in the KO-Sham group, when compared with the WT-Sham group. This was not observed in the study using 3- and 8-month-old animals above (Fig. 2). This could be due to altered mechanisms for the apparent changes in Ca^{2+} handling in the setting of age-related and overload-induced electrophysiological remodelling. There was no change to the LTCC after mechanical overload in KO or WT (Fig. 6). This was also different to the age-related study, again indicating a possible distinct pathway of changes mediating electrophysiological remodelling. The AP was also unaffected in amplitude or time for 50% or 90% depolarization at all frequencies studied (Supplementary Material, Fig. S2), implying that AP changes do not play a role.

Pronounced t-tubule loss and disorder following mechanical overload in Tcap KO

Chronic mechanical overload induces loss and disorder in the t-tubule system, which has been reported in multiple studies (1), and we also found this (Fig. 7). Tcap KO showed a profound loss of t-tubule density and regularity, which was significantly greater than the loss that occurred in WT cells. This implies that Tcap's role in regulating t-tubule structure is particularly important in the setting of mechanical overload.

We examined the cell surface sarcolemma using SICM and found that TAC induced pathological remodelling of the cell membrane surface with loss of the Z-grooves (Fig. 8) in Tcap KOs and obvious loss of the t-tubule openings.

DISCUSSION

This study shows that the loss of Tcap from cardiomyocytes is associated initially with an isolated t-tubule defect, with minor Ca^{2+} handling changes and normal heart and cellular function, suggesting that this effect is important. This defect becomes worse with ageing and is associated with significant changes in Ca^{2+} cycling. During mechanical overload, there is pronounced t-tubule loss and remodelling, indicating that Tcap is necessary to maintain t-tubule structure and function, especially after mechanical overload. These findings are summarized in Table 1.

T-tubule regulation

The t-tubule system maintains the LTCC in close localization with the RyR and promotes efficient CICR (21). This ensures that the signal to release SR Ca^{2+} is spread throughout the

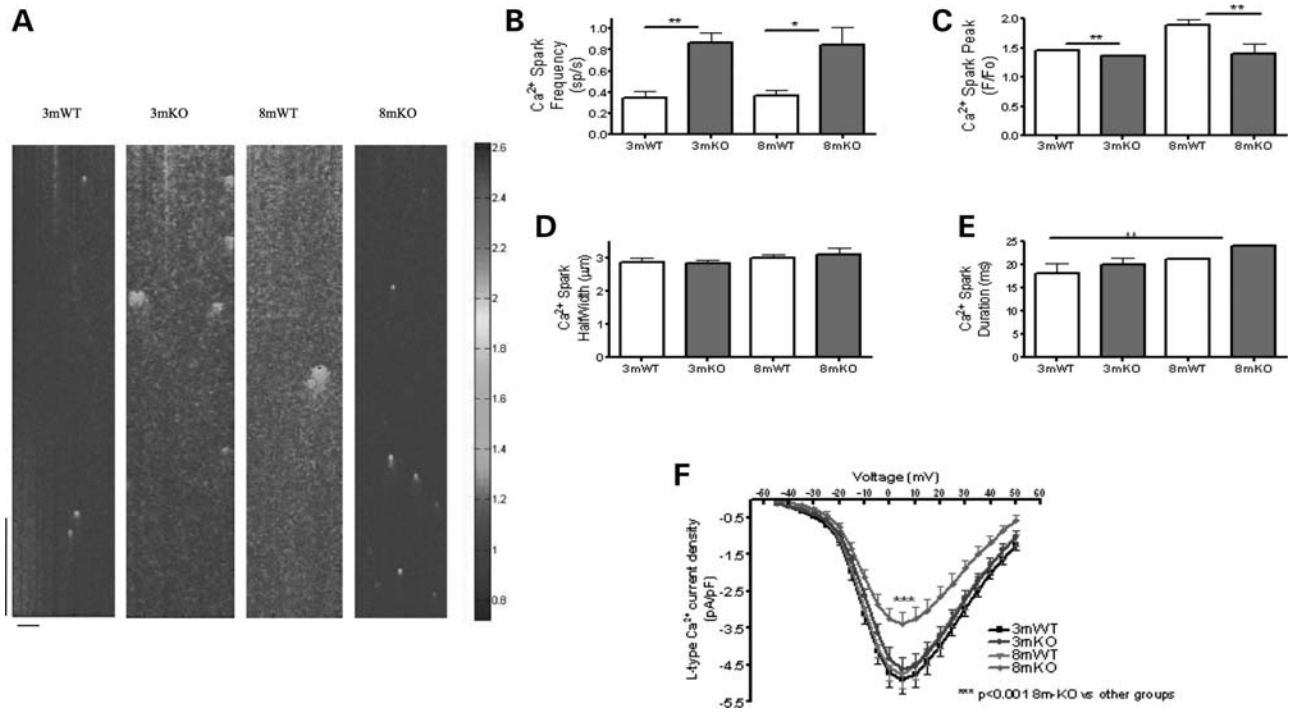

Figure 2. Tcap KO is associated with progressive Ca^{2+} spark and LTCC defects. (**A**) The figure shows line scans of quiescent ventricular cardiomyocytes from 3 month or 8 month WT and Tcap KO hearts. The colour chart is a normalized scale of fluorescence intensity (a marker of Ca^{2+} concentration). 3mWT $n = 40$, 3mKO $n = 48$, 8mWT $n = 48$, 8mKO $n = 43$. The vertical scale bar represents 768 ms and the horizontal scale bar represents 100 pixels. Ca^{2+} spark frequency was increased (**B**) and Ca^{2+} spark peak was reduced (**C**) at 3 and 8 months in the KO. Ca^{2+} spark width (**D**) and duration (**E**) were not significantly changed. (**F**) The L-type Ca^{2+} channel current density is reduced in 8mKO. 3mWT $n = 24$, 3mKO $n = 25$, 8mWT $n = 16$, 8mKO $n = 20$.

whole depth of the cell, promoting synchronous Ca^{2+} transients and contraction. When the t-tubules are lost or disrupted, the RyR are 'orphaned' resulting in impaired CICR (4). Such t-tubule remodelling appears to be an early event in the progression of overload-induced HF (1) and is ubiquitous, irrespective of the aetiology of HF (14).

The t-tubules are regulated by a number of molecules, each acting at different levels. BIN1 is a protein that induces membrane invaginations and is responsible for the biogenesis of t-tubules (7). In addition, BIN1 is responsible for shuttling the LTCC to the t-tubule membrane (6). BIN1 expression is reduced, and LTCC trafficking is impaired in human HF (22). Another molecule, Junctophilin-2 is involved in t-tubule–SR tethering (8) and is reduced proportionally with the progression from hypertrophy to HF (1). Many other molecules may be involved in t-tubule regulation (for a review, see (5)).

A major biophysical regulator of the t-tubule system is mechanical load variation, as both increased (1) and reduced (2) mechanical load can disrupt t-tubule structure, when prolonged. Zhang *et al.* (12) identified Tcap as a load-dependent promoter of t-tubule formation in response to stretch in zebrafish skeletal muscle. We have recently reported that during HF, Tcap expression declines, then recovers after sarcoendoplasmic reticulum ATPase gene therapy-induced reverse remodelling, correlating with observed loss and reappearance of the t-tubules (23). Here, we show that the lack of Tcap results initially in isolated abnormal t-tubule structure, with few Ca^{2+} handling changes (discussed below). This is highly suggestive of an important Tcap-t-tubule regulatory role. In the absence of Tcap, mechanical overload results in pronounced t-tubule dysfunction with major implications for CICR. Taken together, these data suggest that Tcap is involved in the regulation of t-tubule structure, especially after mechanical overload. Whether it is possible to reverse the t-tubule defects caused by the loss of Tcap by the reintroduction of Tcap is not known at present, and should be tested by future studies. Tcap may be tightly regulated by not only its overall expression but potentially also by its subcellular localization and post-translational modification. Further work is needed to elucidate the regulation of Tcap and its utility as a therapeutic agent.

Ca^{2+} handling abnormalities

During excitation–contraction coupling in cardiomyocytes, the AP activates the LTCC throughout the surface and t-tubule membranes, which allows small fluxes of Ca^{2+} to enter the cell and activate the RyR (24). The RyR then releases Ca^{2+} from the SR that activates the contractile apparatus. Every element in this system can be altered causing a change in Ca^{2+} transient morphology and, therefore, contractility. In this study, we systematically analysed the major mechanisms involved.

The AP morphology was unaffected by either lack of Tcap or mechanical overload. The AP can influence CICR (18), but does not appear to play a role in the effects of lack of Tcap or after mechanical overload during the conditions studied here.

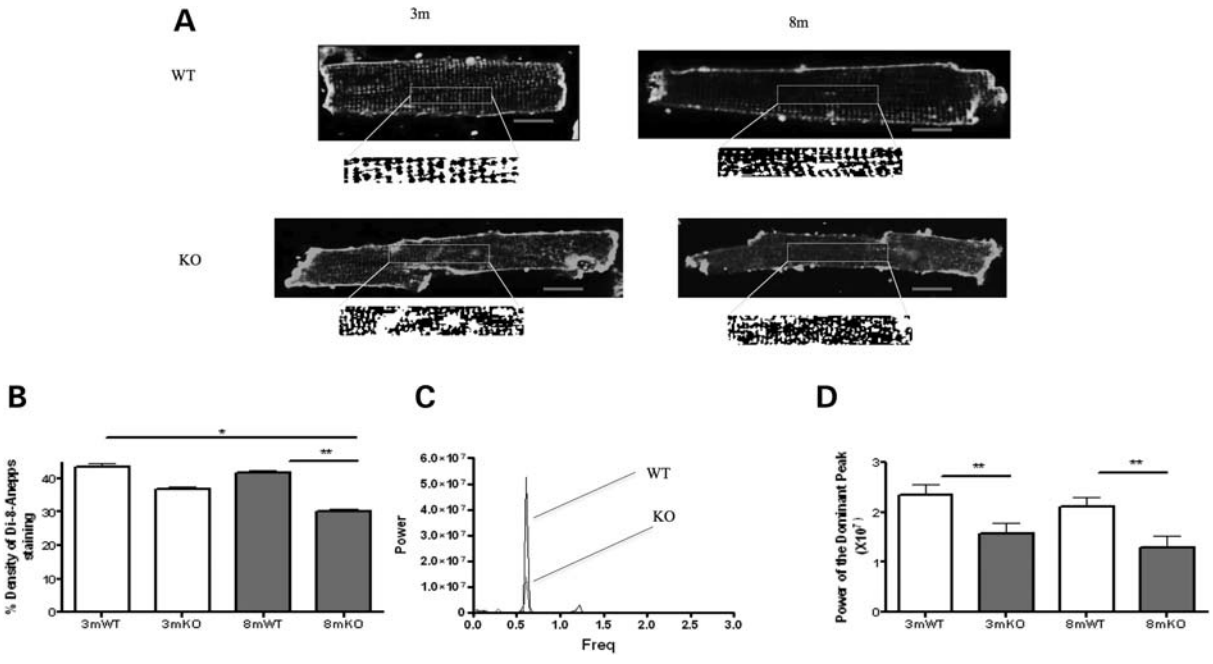

Figure 3. T-tubule structure is disrupted in Tcap KO. (**A**) The figure shows single di-8-ANEPPS-stained cardiomyocytes from which t-tubule density (**B**) and regularity are calculated. (B) T-tubule density is reduced at the 8 month in the KO. The lower box illustrates the analysis of t-tubule regularity with the central portion of cardiomyocytes converted into a binary image that was analysed using Fourier transformation. This provides a power–frequency curve, the peak of which is taken as an index of t-tubule regularity (**C** and **D**). T-tubule regularity is reduced in the KO. 3mWT $n = 30$, 3mKO $n = 32$, 8mWT $n = 45$, 8mKO $n = 44$. Red scale bars represent 10 μm.

The effect on the LTCC is complex. We found that in 8mKO, where t-tubule density was depressed, the LTCC density was also significantly depressed. Such LTCC depression could result in smaller increases in the dyadic [Ca^{2+}], resulting in less Ca^{2+} release from the SR and, therefore, less activation of the contractile apparatus. We did not observe depressed Ca^{2+} transient amplitude, possibly due to compensatory increases in SR Ca^{2+} content, although this needs to be determined. We further found that during conditions of overload in both WT and KO cells, where t-tubule density was also depressed, LTCC density, a measure of LTCC activity normalized to membrane area, was unaffected. This could be due to a proportionally equal loss of membrane area and LTCCs, providing an overall normal value for LTCC density.

In 3mKO, as previously reported (15), the amplitude and duration of the whole-cell Ca^{2+} transient were not different from WT. However, using confocal microscopy, we performed an additional study of CICR synchronicity and found that this was significantly disrupted in 3mKO. The points of delayed Ca^{2+} release spatially colocalize to defects in the t-tubule system, indicating that these areas of dysynchrony are caused by delayed RyR activation due to LTCC-RyR uncoupling (16,25,26). T-tubule morphology is not the only regulator of CICR synchrony, but given that Ca^{2+} handling appears intact at this stage, t-tubule remodelling is likely the cause of this loss of synchrony (18,21). In 8mKO, in addition to the loss of synchronous CICR, there is also prolongation of the time to peak and time for 90% decline of the Ca^{2+} transient. This is accompanied by the loss of t-tubule density, which would further uncouple CICR.

After mechanical overload, Ca^{2+} transient remodelling occurs with a prolongation of the time to peak, loss of Ca^{2+} release synchrony and prolongation (3,5). In myocytes lacking Tcap, mechanical overload induced additional prolongation of the Ca^{2+} transient. One explanation for this effect is that pronounced t-tubule defects in this group result in altered interaction between ion channels responsible for efficient CICR, resulting in severe Ca^{2+} transient remodelling. Interestingly, despite longer Ca^{2+} spark duration after TAC, the Ca^{2+} transient decline was faster in KO when compared with WT Shams. The reasons for this are complex and could be related to Tcap interactions with other receptors and ion channels that we have not studied, including Na^{+}/Ca^{2+} exchanger (NCX) (27).

In 3mKO, Ca^{2+} spark frequency was elevated. Increased Ca^{2+} spark frequency occurs in HF, where the t-tubules are abnormal or missing, (28) and this increased Ca^{2+} spark frequency is spatially localized to gaps in the t-tubule system (16,29,30). Ca^{2+} spark frequency was elevated in KOs, but not WT after TAC, possibly due to the pronounced t-tubule loss, resulting in LTCC-RyR uncoupling. The Ca^{2+} spark duration was prolonged in both WT and KO after TAC. One mechanism that could mediate this is displacement or loss of NCX. Loss of NCX could delay the extrusion of Ca^{2+}, resulting in prolonged Ca^{2+} sparks (31). KO Sham cells showed longer Ca^{2+} spark duration when compared with WT Sham. Ca^{2+} spark duration is a complex parameter and depends on factors promoting Ca^{2+} leak, altering Ca^{2+} diffusion properties throughout the cytoplasm and Ca^{2+} extrusion from the cytoplasm (32). Efficient CICR is mediated by the correct interaction between the L-type Ca^{2+} channel and RyR. The

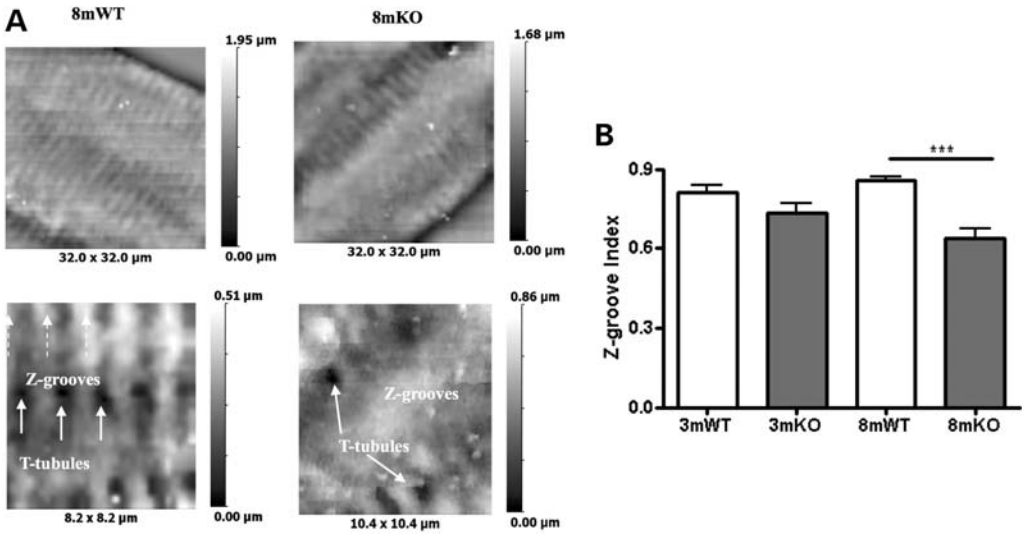

Figure 4. Cell surface structure is disrupted in Tcap KO. (**A**) Low-power (top images) and high-power (bottom images) views of the cell surface of 8 month WT and KO cells are shown. (**B**) The Z-groove provides an index of cell surface regularity, reduced in the KO at the 8 month. 3mWT $n = 7$, 3mKO $n = 16$, 8mWT $n = 30$, 8mKO $n = 20$.

spatial interaction between these two channels plays a significant role in their activation. This relationship is also influenced by primary changes in either channel. The important role of RyR mutations in influencing the progression of HF has been documented extensively (33–36).

Changes to the cell surface

The cell surface of normal ventricular cardiomyocytes is a highly organized and regular structure with a fine architecture consisting of Z-grooves and crests (37). These areas have distinct signalling microdomains that can shift in disease (38). In 3mKO, the cell surface is not altered, but in 8mKO, cell surface remodelling occurs. After mechanical overload, the cell surface is also disrupted. The implications for CICR of Z-groove loss are not clear, although in all conditions studied so far, where Z-groove remodelling has occurred, there are also CICR defects (14). Importantly, the intact cell surface structure of 3mKO indicates that these cells are not in a state of general pathological remodelling and that their gross structural features are intact. Together with previous reports (12), this implies that the t-tubule changes in these cells are an isolated, important defect.

A novel role for Tcap

Tcap is a 19 KDa protein of the sarcomeric Z-disc, which is involved in a class of muscular dystrophies (39). Recent work has suggested that one mechanism by which Tcap mutations result in such muscular dystrophies is by disruption of the t-tubule system (12).

Tcap KO has been studied previously (15,40). These studies show that although Tcap is not essential for skeletal or cardiac muscle development, contractile and stretch-sensing defects occur. In the heart, Tcap KOs show no gross cardiac disease spontaneously (15), but its signalling with p53 results in profound apoptosis after the institution of mechanical overload, with contractile failure. In this study, we show that Tcap is required for normal t-tubule structure at rest, but that this results in few defects to CICR, presumably due to the presence of compensatory mechanisms not studied here. After mechanical overload, Tcap KOs show extensive reduction of t-tubule density and regularity with major Ca^{2+} handling defects that are characteristic of failing ventricular cardiomyocytes (21).

Molecular mechanism mediating Tcap–t-tubule interaction

In the heart, Tcap interacts with a number of proteins to form a stretch-sensing complex (10). Mutations in Tcap can give rise to both hypertrophic and dilated cardiomyopathy, possibly related to altered stretch-sensing properties (13). Importantly, Tcap also binds minK, the regulatory β-subunit of the delayed rectifier potassium current channel, which resides in the t-tubules (11), providing a possible molecular mechanism for the findings observed in this study. This suggests a role for Tcap in coupling stretch sensation with the t-tubule membrane. Zhang *et al.* showed in zebrafish that t-tubule development, which corresponds to body twitch initiation, is dependent on normal Tcap expression (12). Reduction of body movement by anaesthesia delayed t-tubule development. The authors concluded that Tcap could be regulating the t-tubule system in response to changes in stretch. One way in which Tcap could perform mechanosensation functions might be using the integrin-linked kinase system, which should be tested in future studies (41). Tcap may act on the t-tubules via binding to minK. Although this is possible, a number of alternative mechanisms may explain Tcap's regulatory influence over the t-tubules, including signalling via the integrin-linked kinase pathway and altered phosphorylation of binding partners or through the titin kinase domain (42).

With the recent discovery that truncating mutations in titin are a common cause of dilated cardiomyopathy (43), and earlier work documenting Tcap mutations in dilated cardiomyopathy,

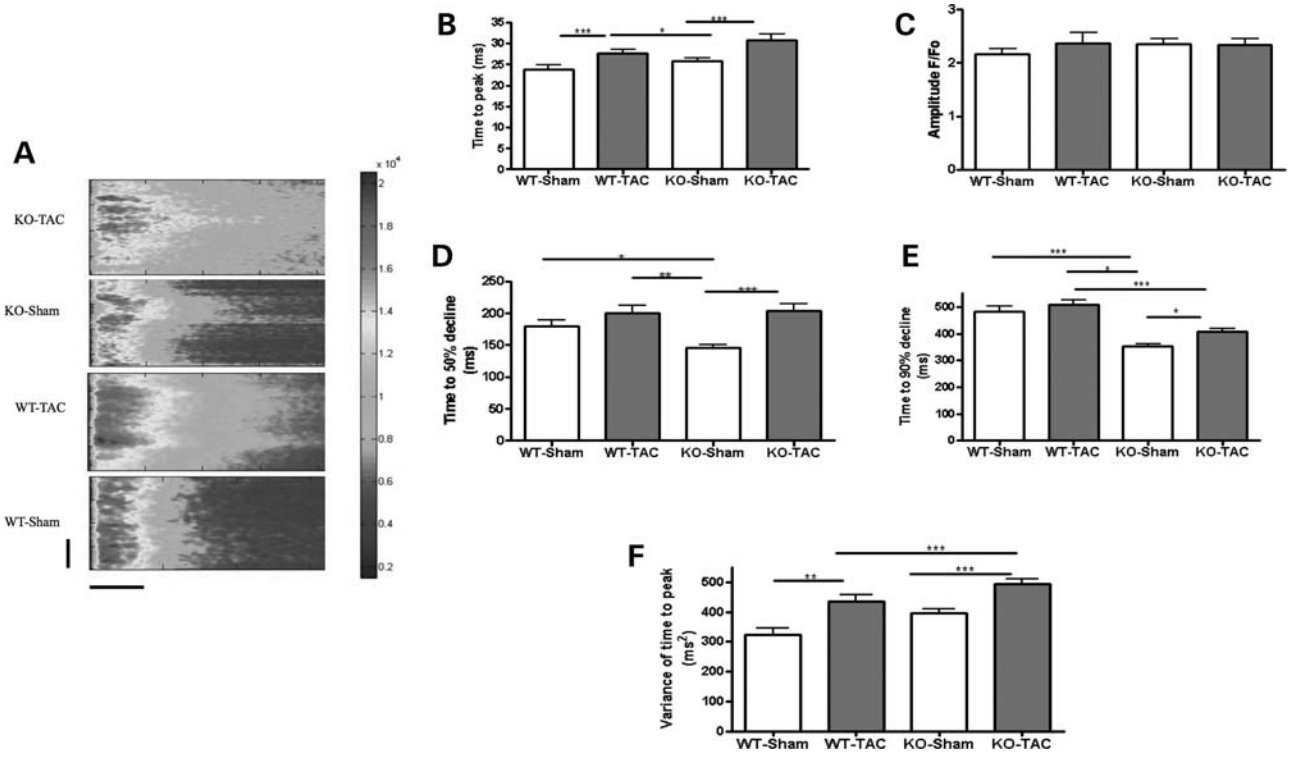

Figure 5. Mechanical overload causes severe Ca^{2+} transient defects in Tcap KO. (**A**) The figure shows line scans of stimulated ventricular cardiomyocytes from Sham or overloaded (TAC) WT and Tcap knock-out (TCAP) hearts. The colour chart is a normalized scale of fluorescence intensity (a marker of Ca^{2+} concentration). WT-Sham $n = 34$, WT-TAC $n = 32$, KO-Sham $n = 31$, KO-TAC $n = 34$. The vertical scale bar represents 100 pixels and the horizontal scale bar represents 100 ms. (**B**) The time to peak of the Ca^{2+} transient was increased in both the WT and KO following TAC, the amplitude was unchanged (**C**) and the time for 50% or 90% decline was increased only in the KO (**D** and **E**). The variance of the time to peak of the Ca^{2+} transient was raised more by TAC in the KO (**F**).

the titin-Tcap axis is emerging as a powerful regulator of cardiac structure and function, in particular in response to mechanical load variation. We have shown that one mechanism by which Tcap acts is via regulation of the t-tubule network. Whether titin shares this action remains to be determined.

Given the large body of evidence showing that the t-tubule system is load sensitive in both myocardial overloading and unloading (1,3,44), we hypothesized that Tcap would regulate the t-tubule system of mammalian ventricular cardiomyocytes in response to load. In this study, we show that myocytes lacking Tcap initially have deranged t-tubule structure with no other defects to the CICR system, suggesting that they are an important defect. When subjected to mechanical overload, the t-tubule system undergoes even more profound remodelling (Table 1), indicating a failure of load-dependent regulation. This supports the hypothesis that Tcap is a critical, load-dependent regulator of t-tubule structure. Further studies are required to elucidate the precise mechanisms mediating the biochemical interactions between Tcap and the t-tubule membrane.

MATERIALS AND METHODS

All procedures were performed according to the guidance of the UK Home Office following ethical review.

Tcap KO mice

Tcap-deficient animals were generated on a C57BL/6 background by replacing the coding regions of exon 1 and 2 by a lacz-neomycin cassette to monitor endogenous gene expression using homologous recombination as described previously (15). To investigate the status of the t-tubule system and local CICR at a young and mature stage, animals were studied at 3 months of age and at 8 months of age. Age- and sex-matched C57BL/6 non-littermate controls were used.

Thoracic aortic constriction

To investigate the impact of chronic mechanical overload, thoracic aortic banding was performed in animals at 8–12 weeks of age. Briefly, animals were anaesthetized by Isoflurane inhalation at 5%, then maintained on 1.5%. A median skin incision was made, and a small portion of the second rib was excised to provide access to the transverse thoracic aorta. A band of 7–0 Prolene was placed under the aorta and tied around a blunted 26 gauge needle, which was later removed. The chest and skin were closed in layers. The animals were recovered and studied 4 weeks after TAC. Sham-operated matched animals were used as controls.

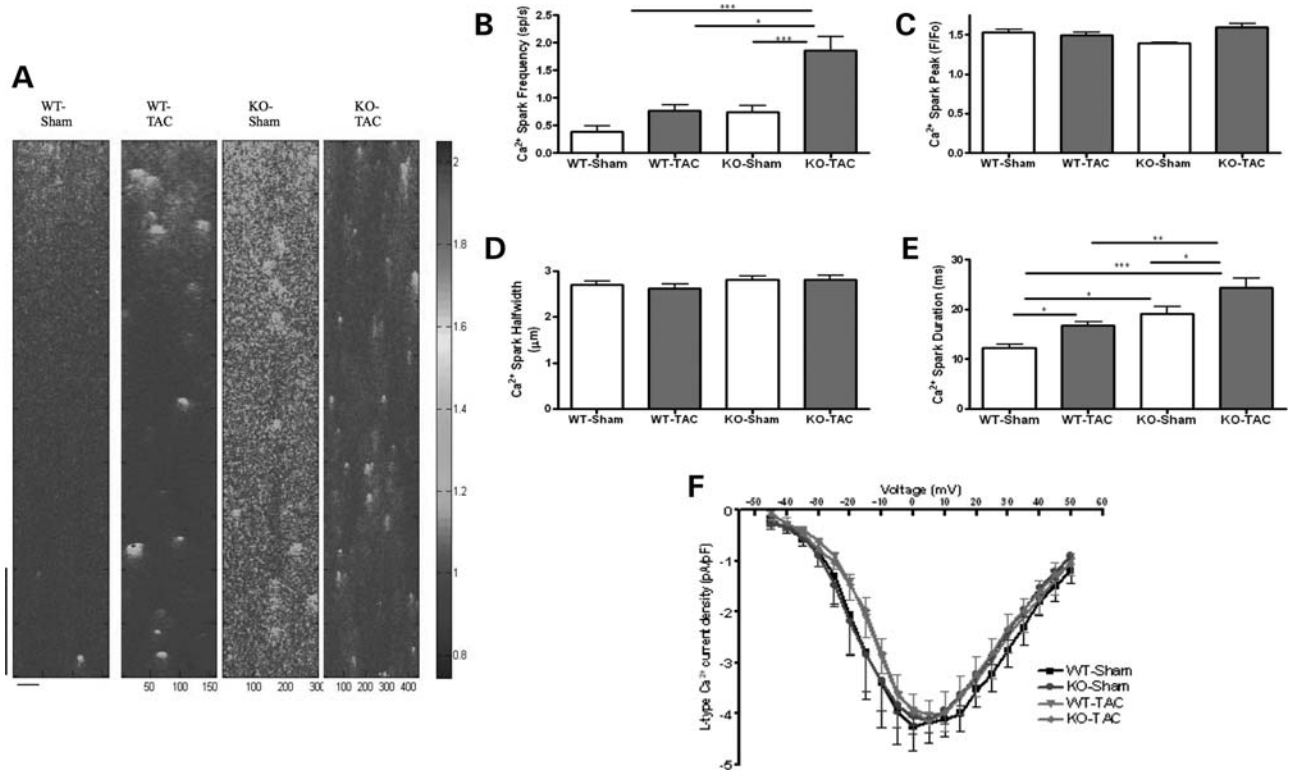

Figure 6. Mechanical overload alters Ca^{2+} spark frequency in Tcap KO, but not WT and does not affect LTCC. (**A**) The figure shows line scans of quiescent ventricular cardiomyocytes. The colour chart is a normalized scale of fluorescence intensity (a marker of Ca^{2+} concentration). WT-Sham $n = 34$, WT-TAC $n = 32$, KO-Sham $n = 31$, KO-TAC $n = 34$. WT-Sham $n = 11$, WT-TAC $n = 16$, KO-Sham $n = 13$, KO-TAC $n = 14$. The vertical scale bar represents 768 ms and the horizontal scale bar represents 100 pixels. (**B**) The Ca^{2+} spark frequency increased only in KO, and Ca^{2+} peak and width did not change (**C** and **D**), whereas the Ca^{2+} spark duration increased more in KOs when compared with WT following TAC (**E**). (**F**) The L-type Ca^{2+} channel current–voltage relationship was unchanged.

Cell isolation

Single left ventricular cardiomyocytes were isolated as described previously (45). All recordings were performed at 37°C with cells superfused with normal Tyrode's solution (140 mM NaCl, 6 mM KCl, 1 mM $MgCl_2$, 1 mM $CaCl_2$, 10 mM glucose and 10 mM HEPES, adjusted to pH 7.4 with 2M NaOH) unless otherwise indicated.

Ca^{2+} handling imaging and electrophysiology

The Ca^{2+}-sensitive fluorescent dye fluo-4 AM (Molecular Probes) was used to monitor local changes in Ca^{2+} concentration. Aliquots of cells were incubated with fluo-4 AM (10 μM) for 20 min, and this mixture was allowed to de-esterify for at least 30 min before cells were used. The experimental chamber was mounted on the stage of a Zeiss Axiovert microscope (Carl Zeiss, Oberkochen, Germany) with an LSM 510 confocal attachment, and myocytes were observed through a Zeiss EC Plan-NeoFluar ×40 oil-immersion lens (numerical aperture 1.3). Excitation was using the 488 nm line of an argon laser, and the emitted fluorescence was collected through a 505 nm long-pass filter. After a period of 30 s of quiescence, line scans were collected. Analysis was performed using custom-written routines in MATLAB R2006b (The MathWorks, Inc., MA, USA), following the threshold-based algorithm for automatic Ca^{2+} spark detection of Cheng *et al.* (46). Detection criteria for Ca^{2+} sparks were set at 3.8 SD above the background noise. Ca^{2+} spark frequency was obtained from the line scans, and Ca^{2+} spark amplitude was defined as the peak fluorescence over background fluorescence (F/F_0). Morphometric analysis of Ca^{2+} sparks elucidated the full width at half-maximum and full duration at half-maximum. To examine the Ca^{2+} transient, cells were field stimulated at 1 Hz, and a line scan was performed, as described previously (2). We measured time to peak, amplitude and variance of time to peak. Time for decline in the Ca^{2+} transient was measured as the time from the peak of the Ca^{2+} transient to 50% or 90% decline.

For AP recordings, cells were studied using an Axon 2B amplifier (Axon Instruments, Union City, CA, USA) in discontinuous (switch clamp) mode. The pipette resistance was ~30 MΩ, and the pipette filling solution contained 2000 mM KCl, 5 mM HEPES and 0.1 mM ethylene glycol tetraacetic acid (EGTA) (pH 7.2). APs were recorded using the perforated patch technique, while the whole-cell configuration of the patch clamp technique was used to record currents. From the voltage measurements, the maximum upstroke velocity, time for 50 and 90% depolarization were measured.

LTCC was measured in voltage-clamp mode as described previously (47). LTCC was measured using a MultiClamp 700A (Axon Instruments, Union City, CA, USA) in whole-cell

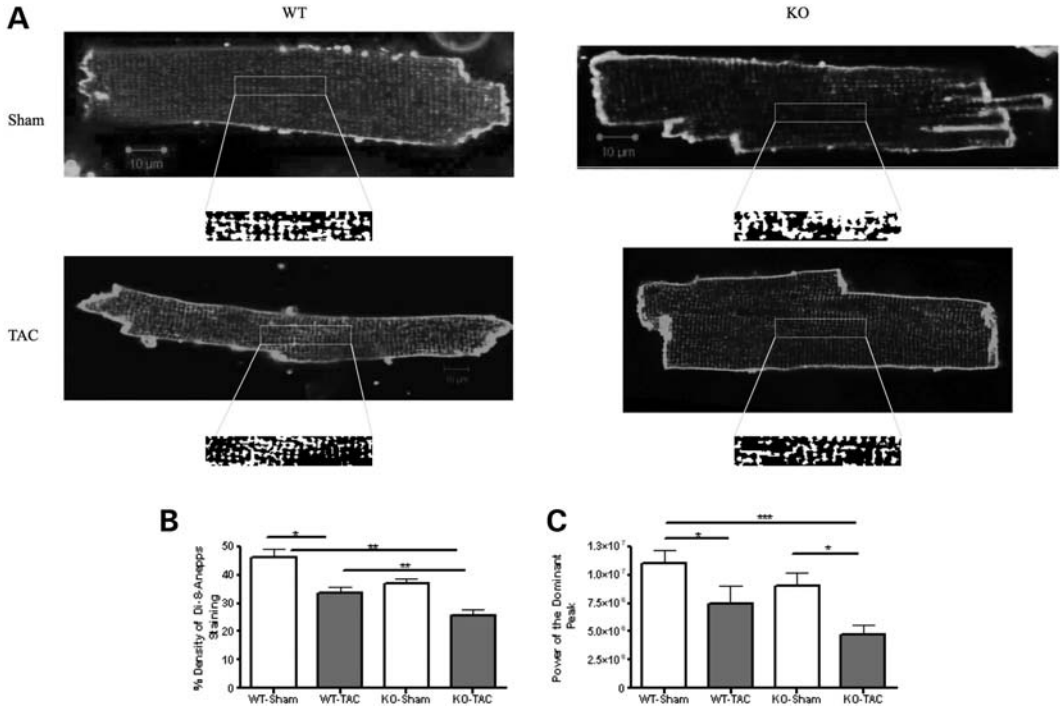

Figure 7. Profound T-tubule loss occurs after mechanical overload in Tcap KO. (**A**) The figure shows single di-8-ANEPPS-stained cardiomyocytes from which t-tubule density (**B**) and regularity are calculated (**C**). WT-Sham $n = 31$, WT-TAC $n = 28$, KO-Sham $n = 30$, KO-TAC $n = 34$. T-tubule regularity is reduced more by TAC in KOs.

patch configuration. The pipette resistance was ~2–3 MΩ, and the pipette-filling solution contained the following: 115 mM Cesium aspartate, 20 mM tetraethylammonium chloride, 10 mM EGTA, 10 mM HEPES and 5 mM MgATP, pH 7.2. The external solution contained the following: 140 mM NaCl, 10 mM glucose, 10 mM HEPES, 1 mM $CaCl_2$, 1 mM $MgCl_2$ and 6 mM CsCl, pH 7.4. Current–voltage relationships for LTCC were built using 450 ms depolarization steps from a holding potential of ~40 mV (range +40 to −40 mV, in 5 mV increments) at 1 Hz. Then, 200 μM Cd^{2+} was applied, and the protocol was repeated. Subtracted currents obtained were normalized to cell capacitance. All experiments were conducted at 37°C.

Imaging of t-tubules and cell surface

The membrane-binding dye, di-8-ANEPPS (Molecular Probes, Eugene, OR, USA), was used. Di-8-ANEPPS (10 μM) was added to a suspension of isolated cells for 10 min, and then washed. Using the same confocal settings as above, a focal plane that excluded the nuclei was selected for high-resolution imaging of the t-tubule structure. Lower resolution Z-stack images of the same cells were used to assess the t-tubule density of cardiomyocytes. The t-tubule density was calculated by converting the Di-8-Anepps signal to a binary signal, using the autothreshold function of ImageJ. After exclusion of the surface sarcolemma, the whole z-series was analysed to provide the percentage stained. This was taken to represent the t-tubule density.

High-resolution images were converted to binary images using the autothreshold function of ImageJ. This involves serial divisions of the 'top' and 'bottom' ends of the range of foreground and background pixel intensities. These binary images were used to generate plot profiles that were analysed in MATLAB (The MathWorks, Inc., Natick, MA, USA) using a custom-written macro to calculate the Fourier transform of the di-8-ANEPPS signal. The peak of the power–frequency relationship was calculated for each image and compared between the control and unloaded groups. The amplitude of the peak is taken as an index of regular distribution of the t-tubule network, as previously described (2). A standard box of 125 × 25 pixels was used and was aligned along the long axis of the cell. The t-tubules should arise at 2 μm intervals, in between sarcomeres. In normal cells, there should be a large, dominant peak in the power–frequency curve, representing the periodic t-tubule striations. When the t-tubules are disrupted or missing, this regular pattern of striations is lost, lowering this peak's power. In figures, cells of different sizes are shown at optimal digital zoom; this results in different numbers of individual t-tubules being shown in the measurement box. However, it is important to note that it is the regularity of the t-tubule striations and not their number that determines the peak of the power–frequency Fourier analysis.

Imaging of cell surface topography using SICM

This uses a micropipette that scans close to the cell surface. The proximity to the cell surface alters the resistance of the pipette and current flow. The changes in current produce an image of the cell surface. In all SICM experiments, micropipettes and the bath solution contained the same physiological L-15 medium (Life Technologies, Inc., Parsley, UK), so that

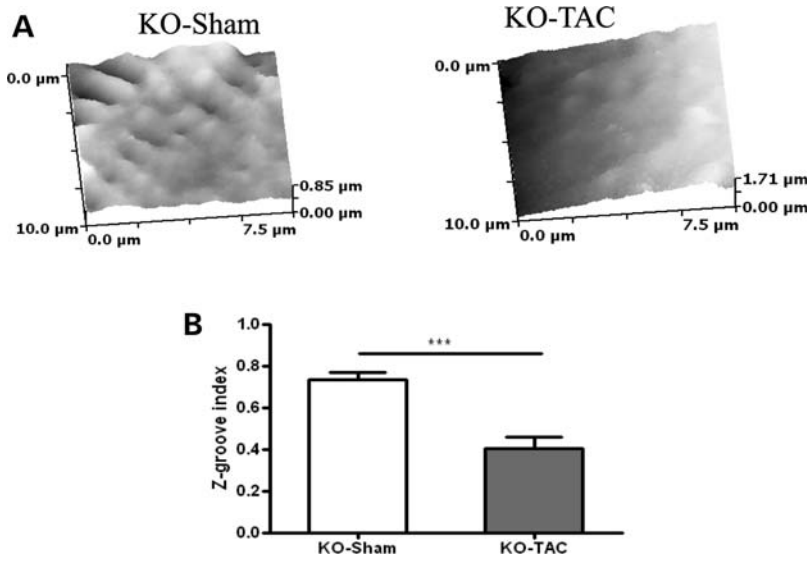

Figure 8. The cell surface structure is disrupted in Tcap KO. (**A**) The cell surface of Tcap KO Sham and TAC cardiomyocytes is shown. (**B**) The cell surface was severely affected by TAC in KOs. KO-Sham $n = 16$, KO-TAC $n = 14$.

Table 1. Summary of key findings in Tcap KOs during ageing and mechanical overload

	Ca^{2+} transient	Ca^{2+} sparks	T-tubules	SICM	L-type Ca^{2+} current	AP
3mKO	↑VTTP	↑Frequency, ↓Peak	↓Reg	NA	NA	NA
8mKO	↑VTTP, ↑TP, ↑T90	↑Frequency, ↓Peak	↓Reg, ↓Density	↓Z-groove	↓	NA
WT TAC	↑VTTP, ↑TTP	↑Duration	↓Reg, ↓Density	–	NA	NA
KO TAC	↑VTTP, ↑TTP, ↑T50, ↑T90	↑Frequency, ↑Duration	↓↓Reg,↓↓Density	↓Z-groove	NA	NA

NA, not applicable; TTP, the time to peak; VTTP, variance of TTP; T50, time for 50% decline; T90, time for 90% decline.

salt concentration gradient potentials and liquid junction potentials were not generated. To quantify the data obtained during scanning, we introduced an index of the completeness of the Z-grooves on the surface of cardiomyocytes (Z-groove index). The Z-groove describes the domes and troughs of the surface of cardiomyocytes, and t-tubule openings are known to sit in these Z-grooves. To calculate the Z-groove index, we measured the maximum extent of Z grooves observed on single SICM images and divided this length by the total estimated Z-groove length, as if they extended across the whole surface, guided by the structure of normal SICM images as described previously (37).

Statistical analysis

Statistical analysis was performed using non-parametric one way ANOVA (Kruskall–Wallis test). Dunn's *post hoc* test was used to test for differences between groups. The analysis was performed using Prism4 software (GraphPad software Inc., San Diego, CA, USA). $P < 0.05$ was taken as significant. *N* numbers refer to the number of cells unless otherwise indicated. Four animals were used in each group.

SUPPLEMENTARY MATERIAL

Supplementary Material is available at *HMG* Online.

Conflicts of Interest: None declared.

FUNDING

M.I. was funded by a British Heart Foundation MB-PhD Grant (FS/09/025/27468). R.K. was supported by DFG Kn 448/9-1, DFG Kn 448 10-1, Fritz Thyssen Stiftung, British Heart Foundation (PG11/34/28793 and RG/11/20/29266) and FP7-PEOPLE-2011-IRSES, Proposal No 291834–Acronym: SarcoSi. M.S. was supported by the Centre of Research Excellence (RE/08/002) and BHF Simon Marks Chair in Regenerative Cardiology (CH/08/002). M.H. was supported by the Banyu Fellowship Program sponsored by Banyu Life Science Foundation International. J.G. was supported by the Wellcome Trust (WTN090594) and the British Heart Foundation (RE/08/002).

REFERENCES

1. Wei, S., Guo, A., Chen, B., Kutschke, W., Xie, Y.P., Zimmerman, K., Weiss, R.M., Anderson, M.E., Cheng, H. and Song, L.S. (2010) T-tubule remodeling during transition from hypertrophy to heart failure. *Circ. Res.*, **107**, 520–531.
2. Ibrahim, M., Al Masri, A., Navaratnarajah, M., Siedlecka, U., Soppa, G.K., Moshkov, A., Al-Saud, S.A., Gorelik, J., Yacoub, M.H. and Terracciano, C.M. (2010) Prolonged mechanical unloading affects

cardiomyocyte excitation-contraction coupling, transverse-tubule structure, and the cell surface. *FASEB J.*, **24**, 3321–3329.
3. Ibrahim, M., Navaratnarajah, M., Siedlecka, U., Rao, C., Dias, P., Moshkov, A.V., Gorelik, J., Yacoub, M.H. and Terracciano, C.M. (2012) Mechanical unloading reverses transverse tubule remodelling and normalizes local Ca(2+)-induced Ca(2+) release in a rodent model of heart failure. *Eur. J. Heart Fail.*, **14**, 571–580.
4. Song, L.S., Sobie, E.A., McCulle, S., Lederer, W.J., Balke, C.W. and Cheng, H. (2006) Orphaned ryanodine receptors in the failing heart. *Proc. Natl. Acad. Sci. USA*, **103**, 4305–4310.
5. Ibrahim, M., Gorelik, J., Yacoub, M.H. and Terracciano, C.M. (2011) The structure and function of cardiac t-tubules in health and disease. *Proc. Biol. Sci.*, **278**, 2714–2723.
6. Hong, T.T., Smyth, J.W., Gao, D., Chu, K.Y., Vogan, J.M., Fong, T.S., Jensen, B.C., Colecraft, H.M. and Shaw, R.M. (2010) BIN1 localizes the L-type calcium channel to cardiac T-tubules. *PLoS Biol.*, **8**, e1000312.
7. Lee, E., Marcucci, M., Daniell, L., Pypaert, M., Weisz, O.A., Ochoa, G.C., Farsad, K., Wenk, M.R. and De Camilli, P. (2002) Amphiphysin 2 (Bin1) and t-tubule biogenesis in muscle. *Science*, **297**, 1193–1196.
8. van Oort, R.J., Garbino, A., Wang, W., Dixit, S.S., Landstrom, A.P., Gaur, N., De Almeida, A.C., Skapura, D.G., Rudy, Y., Burns, A.R. *et al.* (2011) Disrupted junctional membrane complexes and hyperactive ryanodine receptors after acute junctophilin knockdown in mice. *Circulation*, **123**, 979–988.
9. Valle, G., Faulkner, G., De Antoni, A., Pacchioni, B., Pallavicini, A., Pandolfo, D., Tiso, N., Toppo, S., Trevisan, S. and Lanfranchi, G. (1997) Telethonin, a novel sarcomeric protein of heart and skeletal muscle. *FEBS Lett.*, **415**, 163–168.
10. Knöll, R., Hoshijima, M., Hoffman, H.M., Person, V., Lorenzen-Schmidt, I., Bang, M.L., Hayashi, T., Shiga, N., Yasukawa, H., Schaper, W. *et al.* (2002) The cardiac mechanical stretch sensor machinery involves a Z disc complex that is defective in a subset of human dilated cardiomyopathy. *Cell*, **111**, 943–955.
11. Furukawa, T., Ono, Y., Tsuchiya, H., Katayama, Y., Bang, M.L., Labeit, D., Labeit, S., Inagaki, N. and Gregorio, C.C. (2001) Specific interaction of the potassium channel beta-subunit minK with the sarcomeric protein T-cap suggests a T-tubule-myofibril linking system. *J. Mol. Biol.*, **313**, 775–784.
12. Zhang, R., Yang, J., Zhu, J. and Xu, X. (2009) Depletion of zebrafish Tcap leads to muscular dystrophy via disrupting sarcomere-membrane interaction, not sarcomere assembly. *Hum. Mol. Genet.*, **18**, 4130–4140.
13. Hayashi, T., Arimura, T., Itoh-Satoh, M., Ueda, K., Hohda, S., Inagaki, N., Takahashi, M., Hori, H., Yasunami, M., Nishi, H. *et al.* (2004) Tcap gene mutations in hypertrophic cardiomyopathy and dilated cardiomyopathy. *J. Am. Coll. Cardiol.*, **44**, 2192–2201.
14. Lyon, A.R., MacLeod, K.T., Zhang, Y., Garcia, E., Kanda, G.K., Lab, M.J., Korchev, Y.E., Harding, S.E. and Gorelik, J. (2009) Loss of t-tubules and other changes to surface topography in ventricular myocytes from failing human and rat heart. *Proc. Natl. Acad. Sci. USA*, **106**, 6854–6859.
15. Knöll, R., Linke, W.A., Zou, P., Miocic, S., Kostin, S., Buyandelger, B., Ku, C.H., Neef, S., Bug, M., Schafer, K. *et al.* (2011) Telethonin deficiency is associated with maladaptation to biomechanical stress in the mammalian heart. *Circ. Res.*, **109**, 758–769.
16. Heinzel, F.R., Bito, V., Biesmans, L., Wu, M., Detre, E., von Wegner, F., Claus, P., Dymarkowski, S., Maes, F., Bogaert, J. *et al.* (2008) Remodeling of t-tubules and reduced synchrony of Ca2+ release in myocytes from chronically ischemic myocardium. *Circ. Res.*, **102**, 338–346.
17. Cheng, H. and Lederer, W.J. (2008) Calcium sparks. *Physiol. Rev.*, **88**, 1491–1545.
18. Louch, W.E., Hake, J., Jolle, G.F., Mork, H.K., Sjaastad, I., Lines, G.T. and Sejersted, O.M. (2010) Control of Ca2+ release by action potential configuration in normal and failing murine cardiomyocytes. *Biophys. J.*, **99**, 1377–1386.
19. Bailey, B.A. and Houser, S.R. (1992) Calcium transients in feline left ventricular myocytes with hypertrophy induced by slow progressive pressure overload. *J. Mol. Cell Cardiol.*, **24**, 365–373.
20. Xu, M., Zhou, P., Xu, S.M., Liu, Y., Feng, X., Bai, S.H., Bai, Y., Hao, X.M., Han, Q., Zhang, Y. *et al.* (2007) Intermolecular failure of L-type Ca2+ channel and ryanodine receptor signaling in hypertrophy. *PLoS Biol.*, **5**, e21.
21. Louch, W.E., Sejersted, O.M. and Swift, F. (2010) There goes the neighborhood: pathological alterations in t-tubule morphology and consequences for cardiomyocyte Ca2+ handling. *J. Biomed. Biotechnol.*, **2010**, 503906.
22. Hong, T.T., Smyth, J.W., Chu, K.Y., Vogan, J.M., Fong, T.S., Jensen, B.C., Fang, K., Halushka, M.K., Russell, S.D., Colecraft, H. *et al.* (2012) BIN1 is reduced and Cav1.2 trafficking is impaired in human failing cardiomyocytes. *Heart Rhythm*, **9**, 812–820.
23. Lyon, A.R., Nikolaev, V.O., Miragoli, M., Sikkel, M.B., Paur, H., Benard, L., Hulot, J.S., Kohlbrenner, E., Hajjar, R.J., Peters, N.S. *et al.* (2012) Plasticity of surface structures and beta2-adrenergic receptor localization in failing ventricular cardiomyocytes during recovery from heart failure. *Circ. Heart Fail.*, **5**, 357–365.
24. Bers, D.M. (2001) *Excitation-Contraction Coupling and Cardiac Contractile Force*. Kluwer Academic, Dordrecht, Netherlands.
25. Heinzel, F.R., Bito, V., Volders, P.G., Antoons, G., Mubagwa, K. and Sipido, K.R. (2002) Spatial and temporal inhomogeneities during Ca2+ release from the sarcoplasmic reticulum in pig ventricular myocytes. *Circ. Res.*, **91**, 1023–1030.
26. Louch, W.E., Bito, V., Heinzel, F.R., Macianskiene, R., Vanhaecke, J., Flameng, W., Mubagwa, K. and Sipido, K.R. (2004) Reduced synchrony of Ca2+ release with loss of t-tubules–a comparison to Ca2+ release in human failing cardiomyocytes. *Cardiovasc. Res.*, **62**, 63–73.
27. Hussain, M. and Orchard, C.H. (1997) Sarcoplasmic reticulum Ca2+ content, L-type Ca2+ current and the Ca2+ transient in rat myocytes during beta-adrenergic stimulation. *J. Physiol.*, **505**, 385–402.
28. Lyon, A.R., Bannister, M.L., Collins, T., Pearce, E., Sepehripour, A.H., Dubb, S.S., Garcia, E., O'Gara, P., Liang, L., Kohlbrenner, E. *et al.* (2011) SERCA2a gene transfer decreases sarcoplasmic reticulum calcium leak and reduces ventricular arrhythmias in a model of chronic heart failure. *Circ. Arrhythm. Electrophysiol.*, **4**, 362–372.
29. Meethal, S.V., Potter, K.T., Redon, D., Munoz-del-Rio, A., Kamp, T.J., Valdivia, H.H. and Haworth, R.A. (2007) Structure-function relationships of Ca spark activity in normal and failing cardiac myocytes as revealed by flash photography. *Cell Calcium*, **41**, 123–134.
30. Louch, W.E., Mork, H.K., Sexton, J., Stromme, T.A., Laake, P., Sjaastad, I. and Sejersted, O.M. (2006) T-tubule disorganization and reduced synchrony of Ca2+ release in murine cardiomyocytes following myocardial infarction. *J. Physiol.*, **574**, 519–533.
31. Biesmans, L., Macquaide, N., Heinzel, F.R., Bito, V., Smith, G.L. and Sipido, K.R. (2011) Subcellular heterogeneity of ryanodine receptor properties in ventricular myocytes with low t-tubule density. *PLoS One*, **6**, e25100.
32. Zima, A.V., Picht, E., Bers, D.M. and Blatter, L.A. (2008) Termination of cardiac Ca2+ sparks: role of intra-SR [Ca^{2}+], release flux, and intra-SR Ca2+ diffusion. *Circ. Res.*, **103**, e105–e115.
33. Bers, D.M. (2012) Ryanodine receptor S2808 phosphorylation in heart failure: smoking gun or red herring. *Circ. Res.*, **110**, 796–799.
34. Marx, S.O., Reiken, S., Hisamatsu, Y., Jayaraman, T., Burkhoff, D., Rosemblit, N. and Marks, A.R. (2000) PKA phosphorylation dissociates FKBP12.6 from the calcium release channel (ryanodine receptor): defective regulation in failing hearts. *Cell*, **101**, 365–376.
35. Scoote, M. and Williams, A.J. (2002) The cardiac ryanodine receptor (calcium release channel): emerging role in heart failure and arrhythmia pathogenesis. *Cardiovasc. Res.*, **56**, 359–372.
36. Xiao, B., Jiang, M.T., Zhao, M., Yang, D., Sutherland, C., Lai, F.A., Walsh, M.P., Warltier, D.C., Cheng, H. and Chen, S.R. (2005) Characterization of a novel PKA phosphorylation site, serine-2030, reveals no PKA hyperphosphorylation of the cardiac ryanodine receptor in canine heart failure. *Circ. Res.*, **96**, 847–855.
37. Gorelik, J., Yang, L.Q., Zhang, Y., Lab, M., Korchev, Y. and Harding, S.E. (2006) A novel Z-groove index characterizing myocardial surface structure. *Cardiovasc. Res.*, **72**, 422–429.
38. Nikolaev, V.O., Moshkov, A., Lyon, A.R., Miragoli, M., Novak, P., Paur, H., Lohse, M.J., Korchev, Y.E., Harding, S.E. and Gorelik, J. (2010) Beta2-adrenergic receptor redistribution in heart failure changes cAMP compartmentation. *Science*, **327**, 1653–1657.
39. Moreira, E.S., Wiltshire, T.J., Faulkner, G., Nilforoushan, A., Vainzof, M., Suzuki, O.T., Valle, G., Reeves, R., Zatz, M., Passos-Bueno, M.R. *et al.* (2000) Limb-girdle muscular dystrophy type 2G is caused by mutations in the gene encoding the sarcomeric protein telethonin. *Nat. Genet.*, **24**, 163–166.

40. Markert, C.D., Meaney, M.P., Voelker, K.A., Grange, R.W., Dalley, H.W., Cann, J.K., Ahmed, M., Bishwokarma, B., Walker, S.J., Yu, S.X. *et al.* (2010) Functional muscle analysis of the Tcap knockout mouse. *Hum. Mol. Genet.*, **19**, 2268–2283.
41. Knöll, R., Postel, R., Wang, J., Kratzner, R., Hennecke, G., Vacaru, A.M., Vakeel, P., Schubert, C., Murthy, K., Rana, B.K. *et al.* (2007) Laminin-alpha4 and integrin-linked kinase mutations cause human cardiomyopathy via simultaneous defects in cardiomyocytes and endothelial cells. *Circulation*, **116**, 515–525.
42. Gautel, M. (2011) Cytoskeletal protein kinases: titin and its relations in mechanosensing. *Pflugers Arch.*, **462**, 119–134.
43. Herman, D.S., Lam, L., Taylor, M.R., Wang, L., Teekakirikul, P., Christodoulou, D., Conner, L., DePalma, S.R., McDonough, B., Sparks, E. *et al.* (2012) Truncations of titin causing dilated cardiomyopathy. *N. Engl. J. Med.*, **366**, 619–628.
44. Xie, Y.P., Chen, B., Sanders, P., Guo, A., Li, Y., Zimmerman, K., Wang, L.C., Weiss, R.M., Grumbach, I.M., Anderson, M.E. *et al.* (2012) Sildenafil prevents and reverses transverse-tubule remodeling and Ca(2+) handling dysfunction in right ventricle failure induced by pulmonary artery hypertension. *Hypertension*, **59**, 355–362.
45. Siedlecka, U., Arora, M., Kolettis, T., Soppa, G.K., Lee, J., Stagg, M.A., Harding, S.E., Yacoub, M.H. and Terracciano, C.M. (2008) Effects of clenbuterol on contractility and Ca2+ homeostasis of isolated rat ventricular myocytes. *Am. J. Physiol. Heart Circ. Physiol.*, **295**, H1917–H1926.
46. Cheng, H., Song, L.S., Shirokova, N., Gonzalez, A., Lakatta, E.G., Rios, E. and Stern, M.D. (1999) Amplitude distribution of calcium sparks in confocal images: theory and studies with an automatic detection method. *Biophys. J.*, **76**, 606–617.
47. Soppa, G.K., Lee, J., Stagg, M.A., Siedlecka, U., Youssef, S., Yacoub, M.H. and Terracciano, C.M. (2008) Prolonged mechanical unloading reduces myofilament sensitivity to calcium and sarcoplasmic reticulum calcium uptake leading to contractile dysfunction. *J. Heart Lung Transplant.*, **27**, 882–889.